Check for updates

Post-synthetic modification of porous [Cu$_3$(BTC)$_2$] (BTC = benzene-1,3,5-tricarboxylate) metal organic framework with molybdenum and vanadium complexes for the epoxidation of olefins and allyl alcohols

Samira Zamani[1] · Alireza Abbasi[1] · Majid Masteri-Farahani[2]

Abstract

Two metal–organic frameworks (MOFs) were prepared based on post-synthetic modification (PSM) method. To design advanced functional material with enhanced catalytic activity, Cu$_3$(BTC)$_2$ (H$_3$BTC = benzene-1,3,5-tricarboxylate) was synthesized and functionalized with 4-aminopyridine and 2-pyridine carboxaldehyde to achieve a supported bidentate Schiff base. Then, molybdenyl acetylacetonate MoO$_2$(acac)$_2$ and vanadyl acetylacetonate VO(acac)$_2$ were immobilized on Schiff base functionalized Cu$_3$(BTC)$_2$. These newly prepared catalysts were studied by powder X-ray diffraction, Fourier transform infrared spectroscopy (FT-IR), atomic absorption spectroscopy (AAS), field emission scanning electron microscopy (FE-SEM), and also N$_2$ adsorption–desorption (BET method) analyses. After characterization, different parameters influencing the reaction were optimized. A comparative study of the catalytic activity was carried out in the epoxidation of various olefins and allylic alcohols over *tert*-butyl hydroperoxide (TBHP). The maximum conversion was achieved in the case of Mo-catalyst as an effective and selective catalyst in the epoxidation of allylic alcohols.

✉ Alireza Abbasi
aabbasi@khayam.ut.ac.ir

Majid Masteri-Farahani
mfarahani@khu.ac.ir

1 School of Chemistry, College of Science, University of Tehran, Tehran, Iran

2 Faculty of Chemistry, Kharazmi University, Tehran, Iran

Introduction

Although numerous methods for the epoxidation of olefins have been reported [1–6], the preparation of selective and reusable epoxidation catalyst is still an important challenge in synthetic chemistry. Epoxides are important intermediates for the synthesis of various polymers such as polyamides, polyurethanes, etc. [7]. Catalytic epoxidation of olefins as an efficient method to produce an epoxide was utilized in recent decades [8–10]. Metal–organic frameworks (MOFs) have extensively been applied in separation, gas storage, catalysis, and drug delivery [11–13]. A remarkable feature, such as three-dimensional cavities with a high surface area that is easily accessible and enables functionalization of the structure would have numerous merits in the field of catalyst design. The ability of the catalyst for the catalytic process depends on active sites. In other words, a metal-free organic structure or cavity system can act as the active site [14, 15]. The high surface area of MOF provides a higher concentration of active sites per mass which makes the catalysts more efficient [16]. Also, by designing a catalytically active site inside the cavities, a space-size selective catalyst is created [17, 18]. In this regard, porphyrin encapsulated into $Cu_3(BTC)_2$ to prove a size-selective catalyst for epoxidation of an olefin can be mentioned [19]. MOFs are capable of being functionalized with linkers through pre- or post-synthesis modification (PSM) to prepare hybrid materials. Post-synthetic modification refers to the creation of a chemical change in the framework after its synthesis with the preservation of the lattice structure [20]. The advantage of this type of modification is locking and shielding the active sites and avoiding their degradation [21]. An extended network of the MOF can be built by one or multi-metal. If one type of metal involves in the formation of MOF structure, its catalytic activity restricts. Because metal only acts as structure building and doesn't include in catalytic process. Therefore, functionalization with the PSM method is regarded to overcome the drawback and enhances the catalytic activity [22, 23]. Transition-metal compounds with high Lewis acidity and multiple vacancies are good candidates for PSM of MOF. So molybdenyl acetylacetonate and vanadyl acetylacetonate complexes are utilized in this regard. These transition-metals in their high oxidation state i.e. Mo(VI) and V(IV), exhibit excellent Lewis acidity and can act as efficient catalysts. Among various MOFs, $Cu_3(BTC)_2$ has numerous merits in terms of pore design and heterogenization of the compound. Unsaturated copper centers in $Cu_3(BTC)_2$ MOF are believed to be attractive features for modifying and producing hybrid materials. Also, features like a facile synthesis, easy activation, and great surface area make $Cu_3(BTC)_2$ a suitable MOF for post-modification. Herein, we investigated two heterogeneous epoxidation catalysts by anchoring bis(acetylacetonate) oxomolybdenum(VI) and bis(acetylacetonate) oxovanadium(IV) complexes into nanoporous $Cu_3(BTC)_2$ through Schiff-base ligand as a linker. The Schiff base ligand was formed from a two-step connection of 4-aminopyridine and 2-pyridine carbaldehyde inside the cavity by reacting with an unsaturated metal site. The new catalysts were tested in the epoxidation of olefins and allylic alcohol (Scheme 1).
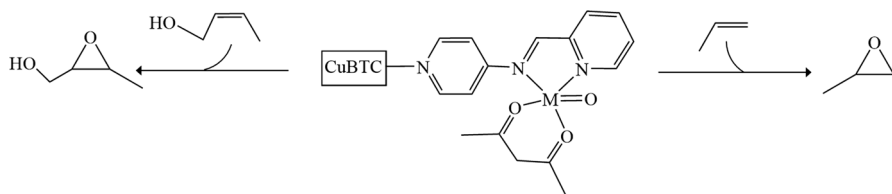
Scheme 1 A model reaction for epoxidation of olefin and allylic alcohol in presence of $Cu_3(BTC)_2$-AMP-PA-M (M = MoO, V)

Experimental Section

The details of used materials and instruments have been included in the supplementary information.

Synthesis of $Cu_3(BTC)_2$ and $Cu_3(BTC)_2$-AMP

$Cu_3(BTC)_2 \cdot nH_2O$ MOF was prepared described by the Kaskel group [24]. $Cu(NO_3)_2 \cdot 3H_2O$ (0.475 g, 1.8 mmol) was dissolved in 6 mL deionized water and added to a solution of trimesic acid (0.21 g, 1.0 mmol) in 6 mL ethanol. The mixture was placed into a Teflon-lined steel autoclave and heated at 120 ˚C for 12 h. The obtained blue crystals were washed several times with ethanol and deionized water, followed by thermal activation at 150 ºC for 24 h to remove anchored H_2O molecules. Afterward, the activated $Cu_3(BTC)_2$ was added to 4-aminopyridine (AMP) (50 mg, 0.54 mmol) in 15 mL dry toluene and stirred under reflux for 16 h to prepare $Cu_3(BTC)_2$-AMP. The final product was isolated, washed four times with ethanol, and then dried for 3 h at 100 °C.

Functionalization of $Cu_3(BTC)_2$

In the first step, $Cu_3(BTC)_2$-AMP synthesized from the previous step was added to a solution of pyridine-2-aldehyde (0.5 mmol, 0.1 g) which dissolved in CH_2Cl_2 (10 mL) and CH_3CN (15 mL). The mixture was allowed to stand (15 days) for the preparation of the Schiff-base ligand. Afterward, $MoO_2(acac)_2$ (16 mg, 0.05 mmol) was dissolved in CH_3CN (5 mL), and the obtained solution was added to the Schiff-base-$Cu_3(BTC)_2$ (200 mg) in CH_3CN (10 mL). The mixture was heated at reflux temperature for 24 h, filtered, and washed with CH_3CN (3 × 10 mL). The prepared sample was activated at 80 °C for 24 h to be used as a heterogeneous catalyst for epoxidation of olefin. The synthetic procedure of the $Cu_3(BTC)_2$-AMP-PA-V is similar to that of the previous catalyst, applying $VO(acac)_2$ (16 mg, 0.05 mmol) instead of $MoO_2(acac)_2$.

Epoxidation of olefins in the presence of prepared catalysts

The catalytic reactions were carried on the 25 mL round-bottomed flask. Typically, 0.5 g of catalyst, was mixed with an olefin (0.008 mol), H_2O_2 (30% in water, 0.014 mol), or *tert*-butyl hydroperoxide (TBHP, 80% in CH_2Cl_2) as an oxidant in chloroform (5 mL). The mixture was refluxed, and the products were monitored by GC. The reusabilities of the catalysts were examined in the cyclooctene epoxidation reaction. The recycling conditions were the same as described above. After each reaction cycle, the catalysts were removed by centrifugation, washed with chloroform and ethanol, then dried under vacuum at 100 °C for 3 h.

Results and discussion

Preparation of heterogeneous catalysts, $Cu_3(BTC)_2$-AMP-PA-Mo and $Cu_3(BTC)_2$-AMP-PA-V

After activation of $Cu_3(BTC)_2$, the unsaturated metal centers will be available to connect to the organic molecules to promote the activity of the structure in catalytic reactions. In the first step, 4-aminopyridine is coordinated covalently to the unsaturated copper centers. The Schiff-base ligand was obtained by post-synthetic covalent modification of $Cu_3(BTC)_2$-AMP, using 2-pyridine carbaldehyde. Subsequently anchoring of Mo(VI) and V(IV) into $Cu_3(BTC)_2$ through complex formation. The proposed structure of supported catalysts is presented in Scheme 2.

Characterization of supported catalysts, $Cu_3(BTC)_2$-AMP-PA-Mo and $Cu_3(BTC)_2$-AMP-PA-V

The FT-IR spectra confirm the successful post-modification process of $Cu_3(BTC)_2$ at each step (Fig. 1). The appeared vibrational peak at 1617 cm^{-1} in the FT-IR spectrum of the $Cu_3(BTC)_2$-AMP (Fig. 1b) can be attributed to the C=N stretching vibration of the pyridine ring in the 4-aminopyridine molecule. Also, The presence of two bands at 3342, 3360 cm^{-1} regions is referred to as the asymmetrical N–H stretch and the symmetrical N–H stretch of NH_2 in 4-aminopyridine. Reduce

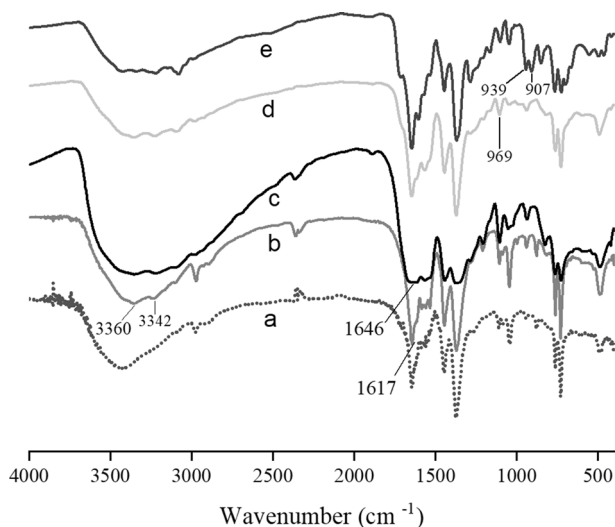**Scheme 2** Overall schematic structure of the catalysts (M = V or MoO)
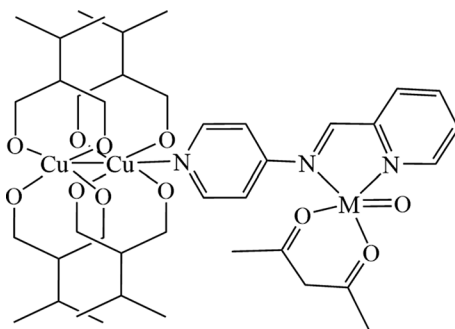
Fig. 1 The FT-IR spectra of $Cu_3(BTC)_2$, and functionalized $Cu_3(BTC)_2$

the intensity of the mentioned bands is related to the alcohol O–H stretches of $Cu_3(BTC)_2$ which is stronger and wider than the corresponding band. the C=N stretching vibration of the imine group is observed at 1646 cm^{-1} after the formation of the Schiff-base ligand, as shown in Fig. 1c. The characteristic peak appeared at 969 in $Cu_3(BTC)_2$-AMP-PA-V and the peaks at 907 and 939 cm^{-1} in $Cu_3(BTC)_2$-AMP-PA-Mo spectra are related to V=O and MoO_2 stretching vibrations, respectively [25, 26] (Figs. 1d, e).

According to the collected data from CHN elemental analysis, the nitrogen amount is increased during the successive steps which demonstrates the successful post-modification process (Table 1). Atomic absorption spectroscopy (AAS) demonstrated the presence of Mo and V with the amount of 0.183 and 0.142 mmol/g for modified catalysts, respectively. The results showed that the loaded amount of $MoO_2(acac)_2$ into the cavities of functionalized $Cu_3(BTC)_2$ is more than $VO(acac)_2$ in the same reaction conditions.

The XRD patterns of $Cu_3(BTC)_2$ and functionalized $Cu_3(BTC)_2$ in the range of $2\theta=10$-60º are shown in Fig. 2. The similarity of $Cu_3(BTC)_2$-AMP-PA-Mo and $Cu_3(BTC)_2$-AMP-PA-V patterns with $Cu_3(BTC)_2$ as synthesized, demonstrate that the framework structure remained intact after modification [27].

Table 1 Elemental analysis results of the samples

Sample	C (%)	H (%)	N (%)
$Cu_3(BTC)_2$	27.77	4.22	–
$Cu_3(BTC)_2$-AMP	37.19	3.23	2.41
$Cu_3(BTC)_2$-AMP-PA	43.01	3.40	3.02

Fig. 2 The XRD patterns of,
a Simulated $Cu_3(BTC)_2$, **b**
as synthesized $Cu_3(BTC)_2$,
c $Cu_3(BTC)_2$-AMP-PA-V, **d**
$Cu_3(BTC)_2$-AMP-PA-Mo
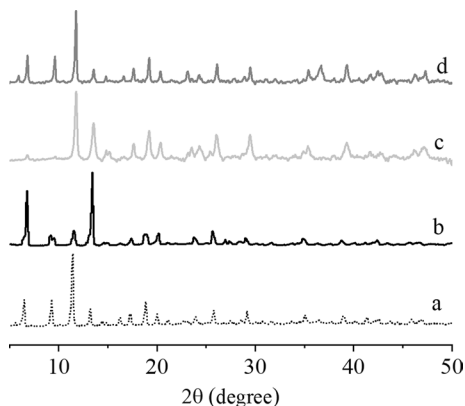
The nitrogen adsorption/desorption isotherms for $Cu_3(BTC)_2$ are depicted in Fig. 3. The $Cu_3(BTC)_2$ exhibits between type I and IV isotherms. This type of isotherm indicates the presence of micropores within the MOF structure. However, the functionalized samples show type II/IV isotherms indicating the pore blocking after modification of parent $Cu_3(BTC)_2$. The BET surface area and total pore volume for $Cu_3(BTC)_2$-AMP-PA-Mo (8.4286 m^2 g^{-1}, 0.05878 cm^3 g^{-1}) and $Cu_3(BTC)_2$-AMP-PA-V (4.489 m^2 g^{-1}, 0.024166 cm^3 g^{-1}) show a remarkable reduction in comparison with parent MOF (1167.6 m^2 g^{-1} and 0.5107 cm^3 g^{-1}) which confirms the successful functionalization.

The SEM images of modified samples were taken to demonstrate the morphology of $Cu_3(BTC)_2$-AMP-PA-V and $Cu_3(BTC)_2$-AMP-PA-Mo, which exhibit octahedral

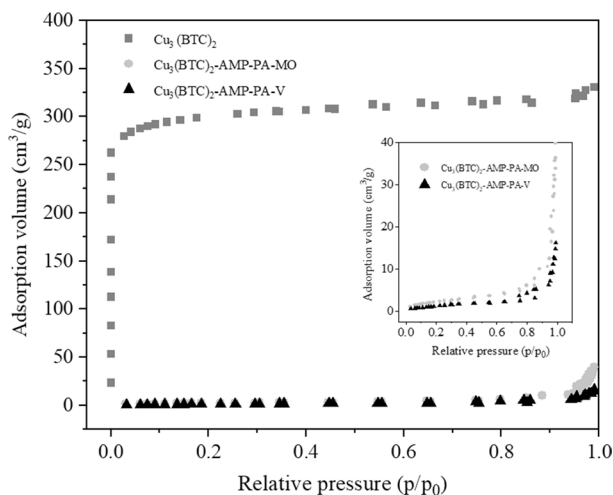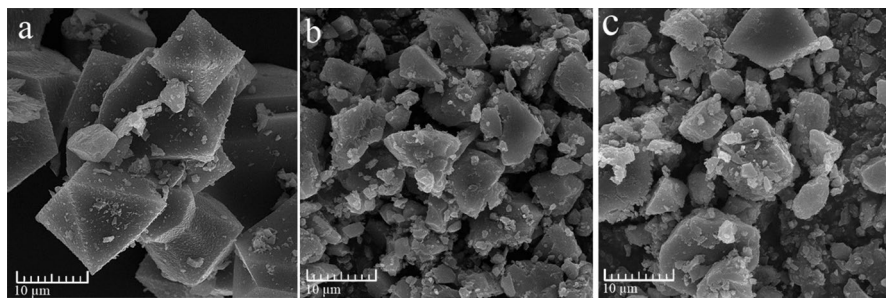**Fig. 3** Nitrogen adsorption–desorption isotherms of prepared materials

Fig. 4 FE-SEM images of **a** $Cu_3(BTC)_2$, **b** $Cu_3(BTC)_2$-AMP-PA-Mo, **c** $Cu_3(BTC)_2$-AMP-PA-V

Table 2 Effect of various solvents in the epoxidation of cyclooctene over $Cu_3(BTC)_2$-AMP-PA-Mo catalyst

Entry	Solvent	Conversion %	Selectivity [a] %
1	$CHCl_3$	100	> 99
2	EtOH	51	61
3	CH_3CN	64	90
4	CH_2Cl_2	32	> 99

Reaction conditions: cyclooctene (0.008mol), TBHP (0.014 mol), catalyst (0.1 g), solvent (5 mL), time (4h). [a]Epoxide selectivity

crystal shapes with the size ranging from 2 to 10 µm. The disruption of the particles shown in Figs. 4b, c compared to Fig. 4a are due to post-synthetic modification of parent $Cu_3(BTC)_2$.

Epoxidation of olefins and allylic alcohol in the presence of $Cu_3(BTC)_2$-AMP-PA-Mo and $Cu_3(BTC)_2$-AMP-PA-V

The effect of various parameters such as time, solvent, type of oxidant, temperature, and the amount of catalyst was explored in the catalytic epoxidation of cyclooctene. The reaction solvent plays an essential role in the efficiency and distribution of epoxidation products. Therefore, the effect of different solvents such as chloroform, ethanol, acetonitrile, and dichloromethane on the conversion reaction was examined. Based on the data in Table 2, chloroform was selected as the optimum solvent in the reaction medium.

The kinetic profile of the cyclooctene epoxidation reaction is shown in Fig. 5. By increasing the reaction time to 3 h, the cyclooctene conversion reaches to its maximum (100%) over $Cu_3(BTC)_2$-AMP-PA-Mo catalyst, while the $Cu_3(BTC)_2$-AMP-PA-V catalyst exhibits lower conversion at this time (79%). This is probably due to the less loading amount of $VO(acac)_2$ on the MOF framework in comparison with $MoO_2(acac)_2$ based on the given data from the AAS technique. Therefore, after evaluating the reaction time, three hours was chosen as the optimal time, and more optimization was performed at this time.

Fig. 5 The kinetic curve of the epoxidation of cyclooctene catalyzed by $Cu_3(BTC)_2$-AMP-PA-Mo and $Cu_3(BTC)_2$-AMP-PA-V. Reaction conditions: cyclooctene (0.008 mol), TBHP (0.014 mol), catalyst (0.1 g), Chloroform (5 mL), reflux
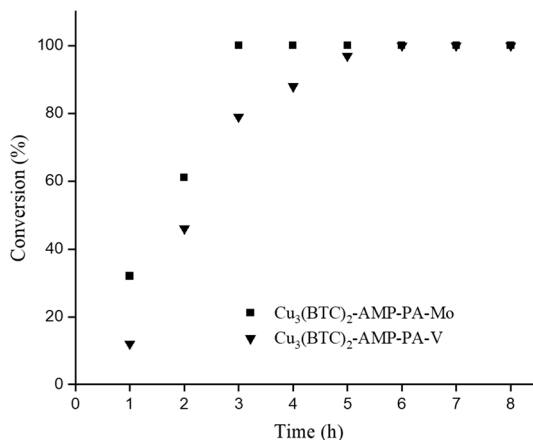
To further optimize, the effect of hydrogen peroxide as oxidant was also investigated. As shown in Fig. 6, the highest conversion was achieved in the presence of TBHP for both heterogeneous catalysts.

The results of the epoxidation of cyclooctene in various conditions are summarized in Table 3. To achieve the optimum temperature, the reaction was performed in the range of 0–120 °C. By increasing the temperature to 90 °C increases the catalytic activity, further rising in temperature decreases leads to the reduction of cyclooctene conversion, because the increasing rate of decomposition of TBHP also affected in conversion value (entries 1–10) [28–38]. Therefore, 90 °C was considered as the optimum temperature for achieving the highest reaction conversion. Finally, since the use of smaller amounts of catalyst in the industrial process is valuable, the catalyst efficiency was evaluated at a lower value. As the result table shows, the activity

Fig. 6 The effect of oxidant on the oxidation of cyclooctene with TBHP. Reaction conditions: cyclooctene (0.008 mol), oxidant (0.014 mol), catalyst (0.1 g), Chloroform (5 mL), time (3 h), reflux
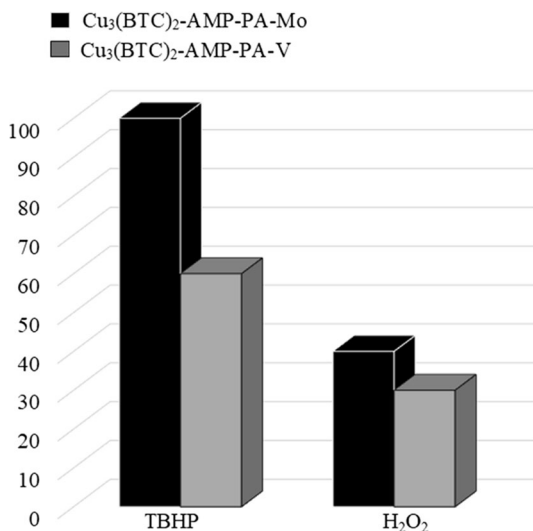
Table 3 The screening of the amount of catalyst and effect of temperature in the epoxidation of cyclooctene in chloroform

Entry	Catalyst	Catalyst amount (g)	Temp (°C)	Conversion[a] (%)	Selectivity[b] (%)
1	$Cu_3(BTC)_2$-AMP-PA-Mo	0.1	0	18	> 99
2	$Cu_3(BTC)_2$-AMP-PA-V	0.1	0	8	> 99
3	$Cu_3(BTC)_2$-AMP-PA-Mo	0.1	25	45	> 99
4	$Cu_3(BTC)_2$-AMP-PA-V	0.1	25	34	> 99
5	$Cu_3(BTC)_2$-AMP-PA-Mo	0.1	60	73	> 99
6	$Cu_3(BTC)_2$-AMP-PA-V	0.1	60	67	> 99
7	$Cu_3(BTC)_2$-AMP-PA-Mo	0.1	90	100	> 99
8	$Cu_3(BTC)_2$-AMP-PA-V	0.1	90	79	> 99
9	$Cu_3(BTC)_2$-AMP-PA-Mo	0.1	120	85	> 99
10	$Cu_3(BTC)_2$-AMP-PA-V	0.1	120	50	> 99
11	$Cu_3(BTC)_2$-AMP-PA-Mo	0.05	90	95	> 99
12	$Cu_3(BTC)_2$-AMP-PA-V	0.05	90	77	> 99

Reaction conditions: cyclooctene (0.008 mol), TBHP (0.014 mol), solvent (5 mL), time (3 h)

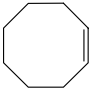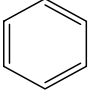[a]GC yield based on initial olefin; [b]Epoxide selectivity
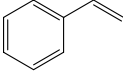
of 0.05 g of catalyst is acceptable to choose as the optimal amount. So, 0.05 g catalyst in the presence of TBHP in 90 °C temperature was chosen as the optimum condition for cyclooctene epoxidation (entries 11–12, 7–8).

Furthermore, epoxidation of various olefins and allylic alcohols with TBHP was carried out over $Cu_3(BTC)_2$-AMP-PA-Mo and $Cu_3(BTC)_2$-AMP-PA-V under the optimized reaction conditions. As seen in Table 4, by increasing the electron density of double bonds in olefins, more epoxidation conversion was achieved. Hence, the reactivity of cyclooctene and cyclohexene are higher than corresponding linear olefins. Also, the different reactivity of allylic alcohols in the epoxidation reaction is affected by the hydroxyl group adjacent to the double bond.

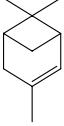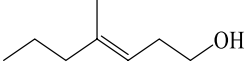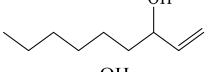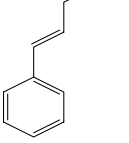Typically, the recovery of the catalysts has been considered an essential industrial property. To check the reusability of the prepared materials, the catalysts were separated after each reaction run, washed twice with chloroform and ethanol, and dried in air. The recycled catalysts were activated at 100 °C to be used in further catalytic cycles (Fig. 7). The reusability of the catalysts was examined in the epoxidation of cyclooctene. The reactivity of $Cu_3(BTC)_2$-AMP-PA-Mo catalyst did not decrease after five recycle runs. In contrast, the significant decrease in reactivity of $Cu_3(BTC)_2$-AMP-PA-V is related to the leaching of the catalyst during each reaction run.

Table 5 shows some reported heterogeneous catalysts containing different solid supports for molybdenum or vanadium species. It can be noticed that a higher formation of epoxy cyclooctane was attained in a shorter reaction time in the presence of $Cu_3(BTC)_2$-AMP-PA-Mo and $Cu_3(BTC)_2$-AMP-PA-V catalysts. This remarkable behavior can be related to the applied support and kind of the donor `atom of chelate. The $Cu_3(BTC)_2$ framework as catalyst shows more reactivity compared to the

Table 4 Epoxidation of various olefins and allylic alcohols in the presence of $Cu_3(BTC)_2$-AMP-PA-Mo and $Cu_3(BTC)_2$-AMP-PA-V

Entry	Substrate	Conversion (%)	
		Cu_3BTC_2-AMP-PA-Mo	Cu_3BTC_2-AMP-PA-V
1		95[a] (>99)	77[a] (>99)
2		80[b] (>99)	78[b] (>99)
3		89[a] (>99)	87[a] (>99)
4		63[b] (>99)	57[b] (>99)
5		90[a] (>99)	75[a] (>99)
6		33[a] (50)	55[a] (66)
7		70[a] (>99)	91[a] (>99)
8		20[a] (50)	94[a] (>99)
9		86[a] (>99)	84[a] (>99)

Reaction conditions: olefin or allyl alcohol (0.008 mol), TBHP (0.014 mmol), catalyst (0.05 g), solvent (5 mL) 90 °C, [a]3 h, [b]24 h. The percentage of epoxide is specified in brackets

other solid supports including graphene oxide (GO), reduced graphene oxide (r-GO) [39], multi-wall carbon nanotube (MWCNT) [40], and magnetic nanoparticles [41]. Also, the crystalline and regular structure of the MOF can prevent the deactivation of the catalytic sites through aggregation. Comparison of epoxidation reactions for catalysts with different donor atoms in Schiff base groups immobilized on similar support [25], indicates that the compounds containing N-donor Schiff bases are more active than those possessing O-donor ligands. This phenomenon can be due to the different electronic effects of N and O donor atoms of the chelating Schiff base
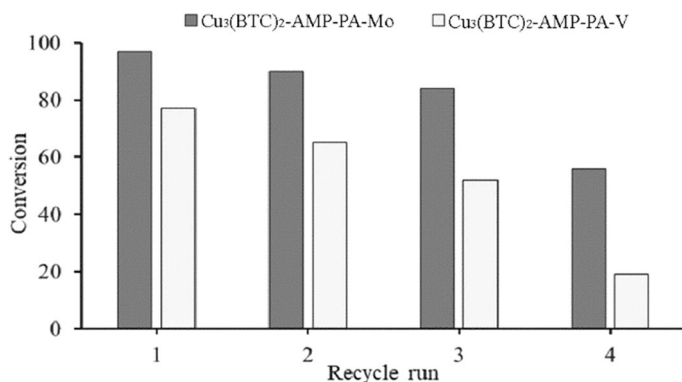
Fig. 7 The reusability of the catalysts. Reaction conditions: cyclooctene (0.008 mol), TBHP (0.014 mmol), catalyst (0.05 g), solvent (5 mL), time (3 h)

and different abilities to stabilizing the metal in various oxidation states [45]. Also, the N donor ligands are more capable than the O donor ones for stabilizing the oxidation state of metal atoms which leads to the reduction of their polarity based on Tweedy's theory [46].

Proposed epoxidation mechanism

The epoxidation mechanism by $Cu_3(BTC)_2$-AMP-PA-V catalyst

Scheme 3 illustrates a proposed catalytic cycle for the epoxidation of olefin and allyl alcohol with TBHP in the presence of $Cu_3(BTC)_2$-AMP-PA-V catalyst. There are various possibilities for the generation of active species, which can be dependent on the substrate. In the case of olefins, first, the $VO(acac)_2$ interacts with TBHP to form the activated complex I, while the simultaneous attack of TBHP and allyl alcohol to the vanadium complex generates the activated complex II. In both cases, vanadium is in its high oxidation state (V^{+5}). Second, the electrophilic attack of the oxygen atom of activated complexes to the double bond of olefin or allyl alcohol produces the epoxides. Complex II is more active than complex I and facilitates the epoxide formation in the presence of allylic alcohol consisting of the electrophilic oxygen atom. Accurately, the hydroxyl group of allylic alcohol adjacent to the double bond makes the transformation of electrophilic oxygen to the double bond much easier [47].

The epoxidation mechanism by $Cu_3(BTC)_2$-AMP-PA-Mo catalyst

In contrast to the previous mechanism, in the epoxidation mechanism of olefin and allylic alcohol by $Cu_3(BTC)_2$-AMP-PA-Mo, only one active species is achieved by the reaction of TBHP with Mo complex, which leads to the formation of molybdenum alkyl peroxide (Scheme 4). The oxygen atom in hydroperoxide is more electrophilic to attack the double bond and as a consequence, more nucleophilic bonds

Table 5 Comparison of the catalytic activity of cyclooctene epoxidation in the presence of several heterogeneous catalyst

Entry	Catalyst	Mol%	Solvent	Time (h)	Con. (%)	Ref
1	GO-Mo	0.3	Chloroform	8	92	[39]
2	rGO-Mo	0.13	Chloroform	8	95	[39]
3	$MoO_2(acac)_2$-sal-MWCNT	0.062	Chloroform	8	99	[40]
4	MoO_2–thio-SCMNPs	0.077	Chloroform	8	100	[41]
5	Mo-thio-Amp-Go	0.137	Chloroform	8	95	[42]
6	Uio_{66}-Sal-Mo	0.122	Acetonitrile	24	90	[43]
7	Mo@UiO-67mixed	1	decane	4	100	[3]
8	Fe_3O_4@SiO_2@Mel-Naph-VO complex	0.12	Acetonitrile	8	80	[44]
9	$Cu_3(BTC)_2$-AMP-PA-Mo	0.114	Chloroform	3	95	This work
10	$Cu_3(BTC)_2$-AMP-PA-V	0.088	Chloroform	3	77	This work
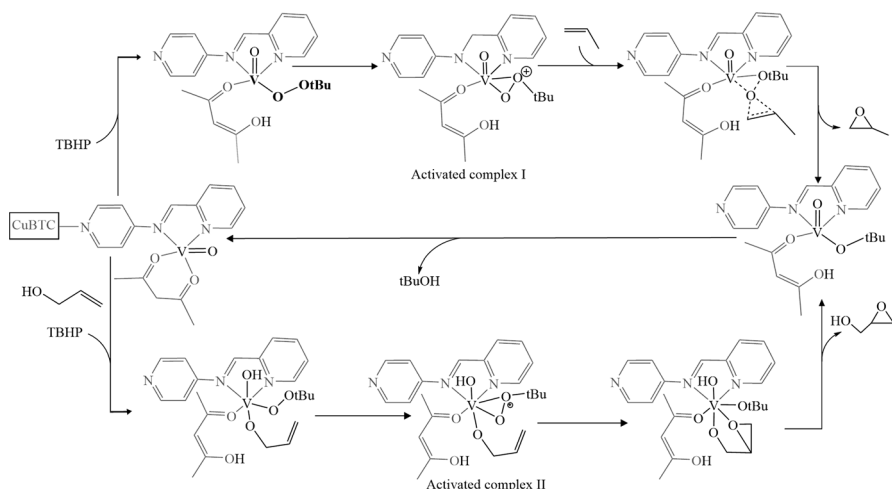
Scheme 3 Suggested mechanism for epoxidation reaction over Cu$_3$(BTC)$_2$-AMP-PA-V
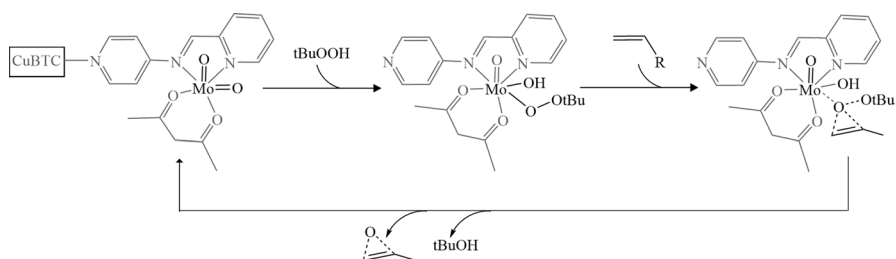
Scheme 4 Suggested mechanism for epoxidation reaction over Cu$_3$(BTC)$_2$-AMP-PA-Mo

facilitate the epoxide formation. In other words, Cu$_3$(BTC)$_2$-AMP-PA-Mo is a more proper catalyst in the olefin epoxidation in comparison with allyl alcohol. In both mechanisms, *tert*-butyl-hydroperoxide has been coordinated to transition metal complexes to generate M-OOH species, in which the active catalysts act as a Lewis acid. The Lewis acidity of metal complexes increases with increasing the oxidation state of metal complexes [48]. Therefore, Mo(VI) is expected to be the most effective catalyst for olefin epoxidation [49].

Conclusions

In summary, two new heterogeneous catalysts were synthesized using the post-synthetic modification method. In this regard, the stable and porous Cu$_3$(BTC)$_2$ was functionalized with 4-aminopyridine and 2-pyridine carboxaldehyde to prepare the Schiff base compound. Then, the MoO$_2$(acac)$_2$ and VO(acac)$_2$ as homogeneous

active catalyst were loaded on the supported Schiff base to prepare efficient heterogenous catalysts for olefins and allylic alcohols epoxidation with TBHP. The $Cu_3(BTC)_2$-AMP-PA-Mo catalyst exhibited significant catalytic performance in the olefin epoxidation, while the $Cu_3(BTC)_2$-AMP-PA-V catalyst was more active in the allylic alcohol epoxidation. Also, our synthesized catalyst showed high activity in the epoxidation reaction compared to other reported solid supports with similar active sites. The easy recovery of catalysts and their subsequent reusability for five catalytic cycles under mild conditions make them useful for industrial processes.

References

1. Al Zoubi W, Al-Hamdani AAS, Kaseem M (2016) Synthesis and antioxidant activities of Schiff bases and their complexes: a review. Appl Organomet Chem 10:810–817
2. Hauser SA, Cokoja M, Kühn FE (2013) Epoxidation of olefins with homogeneous catalysts–quo Vadis? Catal Sci Technol 3:552–561
3. Kaposi M, Cokoja M, Hutterer CH, Hauser SA, Kaposi T, Klappenberger F, Pöthig A, Barth JV, Herrmann WA, Kühn FE (2015) Immobilisation of a molecular epoxidation catalyst on UiO-66 and-67: the effect of pore size on catalyst activity and recycling. Dalton Trans 36:15976–15983
4. Pereira C, Pereira AM, Quaresma P, Tavares PB, Pereira E, Araújo JP, Freire C (2010) Superparamagnetic γ-Fe2O3@SiO2 nanoparticles: a novel support for the immobilization of [VO (acac)2]. Dalton Trans 11:2842–2854
5. Venturello C, Alneri E, Ricci M (1983) A new, effective catalytic system for epoxidation of olefins by hydrogen peroxide under phase-transfer conditions. J Org Chem 21:3831–3833
6. Mohammadikish M, Hashemi SH (2019) Functionalization of magnetite–chitosan nanocomposite with molybdenum complexes: new efficient catalysts for epoxidation of olefins. J Mater Sci 54:6164–6173
7. Manangon-Perugachi LE, Vivian A, Eloy P, Debecker DP, Aprile C, Gaigneaux EM (2019) Hydrophobic titania-silica mixed oxides for the catalytic epoxidation of cyclooctene. Catal Today. https://doi.org/10.1016/j.cattod.2019.05.020
8. Bernar I, Rutjes FP, Elemans JA, Nolte RJ (2019) Aerobic Epoxidation of Low-Molecular-Weight and Polymeric Olefins by a Supramolecular Manganese Porphyrin Catalyst. J Catal 2:195
9. Engelmann X, Malik DD, Corona T, Warm K, Farquhar ER, Swart M, Nam W, Ray K (2019) Trapping of a highly reactive oxoiron (IV) complex in the catalytic epoxidation of olefins by hydrogen peroxide. Angew Chem 12:4052–4056
10. Zhou W, Zhou J, Chen Y, Cui A, He M, Xu Z, Chen Q (2017) Metallophthalocyanine intercalated layered double hydroxides as an efficient catalyst for the selective epoxidation of olefin with oxygen. Appl Catal A: General 542:191–200
11. Bahrani S, Hashemi SA, Mousavi SM, Azhdari R (2019) Zinc-based metal–organic frameworks as nontoxic and biodegradable platforms for biomedical applications: review study. Drug Metab Rev 3:356–377
12. Dawson R, Cooper AI, Adams DJ (2012) Nanoporous organic polymer networks. Prog Polym Sci 4:530–563
13. Hu M-L, Morsali A, Aboutorabi L (2011) Lead (II) carboxylate supramolecular compounds: Coordination modes, structures, and nano-structures aspects. Coord Chem Rev 23–24:2821–2859
14. Lee J, Farha OK, Roberts J, Scheidt KA, Nguyen ST, Hupp JT (2009) Metal-organic framework materials as catalysts. Chem Soc Rev 5:1450–1459

15. Lee JY, Roberts JM, Farha OK, Sarjeant AA, Scheidt KA, Hupp JT (2009) Synthesis and gas sorption properties of a metal-azolium framework (MAF) material. Inorg Chem 21:9971–9973
16. Liang J, Liang Z, Zou R, Zhao Y (2017) Heterogeneous catalysis in zeolites, mesoporous silica, and metal-organic frameworks. Adv Mater 30:1701139
17. Banerjee M, Das S, Yoon M, Choi HJ, Hyun MH, Park SM, Seo G, Kim K (2009) Postsynthetic modification switches an achiral framework to catalytically active homochiral metal-organic porous materials. J Am Chem Soc 22:7524–7525
18. Dang D, Wu P, He C, Xie Z, Duan C (2010) Homochiral metal-organic frameworks for heterogeneous asymmetric catalysis. J Am Chem Soc 41:14321–14323
19. Zhang Z, Zhang L, Wojtas L, Eddaoudi M, Zaworotko MJ (2012) Template-directed synthesis of nets based upon octahemioctahedral cages that encapsulate catalytically active metalloporphyrins. J Am Chem Soc 2:928–933
20. Butova VVe, Soldatov MA, Guda AA, Lomachenko KA, Lamberti C, (2016) Metal-organic frameworks: structure, properties, methods of synthesis, and characterization. Russ Chem Rev 3:280
21. Wang Z, Cohen SM (2009) Postsynthetic modification of metal-organic frameworks. Chem Soc Rev 5:1315–1329
22. Henschel A, Gedrich K, Kraehnert R, Kaskel S (2008) Catalytic properties of MIL-101. Chem Commun 35:4192–4194
23. Janiak C, Vieth JK (2010) MOFs, MILs, and more: concepts, properties, and applications for porous coordination networks (PCNs). New J Chem 11:2366–2388
24. Schlichte K, Kratzke T, Kaskel S (2004) Improved synthesis, thermal stability, and catalytic properties of the metal-organic framework compound Cu3(BTC)2. Microporous Mesoporous Mater 1–2:81–88
25. Guo Y, Xiao L, Li P, Zou W, Zhang W, Hou L (2019) Binuclear molybdenum Schiff-base complex: An efficient catalyst for the epoxidation of alkenes. J Mol Catal 475:110498
26. Wang Z, Cohen SM (2007) Postsynthetic covalent modification of a neutral metal-organic framework. J Am Chem Soc 41:12368–12369
27. Shultz AM, Sarjeant AA, Farha OK, Hupp JT, Nguyen ST (2011) Post-synthesis modification of a metal-organic framework to form metallosalen-containing MOF materials. J Am Chem Soc 34:13252–13255
28. Dl A, Mill T, Dg H, Fr M (1968) Low-Temperature Gas-and Liquid-Phase Oxidations of Isobutane. In: Mayo FR (ed) Oxidation of Organic Compounds Volume II Gas-Phase Oxidations, Homogeneous and Heterogeneous Catalysis Applied Oxidations and Synthetic Processes. ACS Publications, USA
29. De C (2001) Peroxides and peroxide-forming compounds. J Chem Health Saf 5:12–22
30. Ghosh R, Son Y-C, Makwana VD, Suib SL (2004) Liquid-phase epoxidation of olefins by manganese oxide octahedral molecular sieves. J Catal 2:288–296
31. Hiatt RR, Mill T, Irwin KC, Castleman JK (1968) Homolytic decompositions of hydroperoxides. III. Radical-induced decompositions of primary and secondary hydroperoxides. J Org Chem 4:1428–1430
32. Liu H, Gu L, Zhu P, Liu Z, Zhou B (2012) Evaluation on the thermal hazard of ter-butyl hydroperoxide by using accelerating rate calorimeter. Procedia Eng 45:574–579
33. Petrov L, Solyanikov V (1980) Decomposition of tert-butyl hydroperoxide in acetonitrile catalyzed by antimony pentachloride. Bulletin of the Academy of Sciences of the USSR. Chem Sci 7:1081–1086
34. Sanchez J, Myers TN (2005) Peroxides and Peroxide Compounds (Organic). In: Glenn D (ed) Van Nostrand's Encyclopedia of Chemistry. Wiley, Hoboken NJ
35. Wang YW, Duh YS, Shu CM (2007) Characterization of the self-reactive decomposition of tert-butyl hydroperoxide in three different diluents. Process Saf Prog 4:299–303
36. Willms T, Kryk H, Oertel J, Hempel C, Knitt F, Hampel U (2019) On the thermal decomposition of tert.-butyl hydroperoxide, its sensitivity to metals and its kinetics, studied by thermoanalytic methods. Thermochim Acta 672:25–42
37. Willms T, Kryk H, Oertel J, Lu X, Hampel U (2017) Reactivity of t-butyl hydroperoxide and t-butyl peroxide toward reactor materials measured by a microcalorimetric method at 30 °C. J Therm Anal Calorim 1:319–333
38. Winkler D, Hearne G (1961) Liquid phase oxidation of isobutane. J Ind Eng Chem 8:655–658

39. Masteri-Farahani M, Mirshekar S (2018) Covalent functionalization of graphene oxide with molybdenum-carboxylate complexes: new reusable catalysts for the epoxidation of olefins. Colloids Surf A Physicochem Eng Asp 538:387–392

40. Masteri-Farahani M, Abednatanzi S (2013) Immobilized molybdenum–Schiff base complex on the surface of multi-wall carbon nanotubes as a new heterogeneous epoxidation catalyst. Inorg Chem Commun 37:39–42

41. Mohammadikish M, Masteri-Farahani M, Mahdavi S (2014) Immobilized molybdenum–thiosemicarbazide Schiff base complex on the surface of magnetite nanoparticles as a new nanocatalyst for the epoxidation of olefins. J Magn Magn Mater 354:317–323

42. Masteri-Farahani M, Ghahremani M (2019) Surface functionalization of graphene oxide and graphene oxide-magnetite nanocomposite with molybdenum-bidentate Schiff base complex. J Phys Chem Solids 106:6–12

43. Tang J, Dong W, Wang G, Yao Y, Cai L, Liu Y, Zhao X, Xu J, Tan L (2014) Efficient molybdenum (VI) modified Zr-MOF catalysts for epoxidation of olefins. RSC Advances 81:42977–42982

44. Farzaneh F, Asgharpour Z (2019) Synthesis of a new schiff base oxovanadium complex with melamine and 2-hydroxynaphtaldehyde on modified magnetic nanoparticles as catalyst for allyl alcohols and olefins epoxidation. Appl Organomet Chem 5:e4896

45. Kostova I, Saso L (2013) Advances in research of Schiff-base metal complexes as potent antioxidants. Curr Med Chem 36:4609–4632

46. Abou-Hussein AA, Linert W (2014) Synthesis, spectroscopic, coordination and biological activities of some organometallic complexes derived from thio-Schiff base ligands. Spectrochim Acta A 117:763–771

47. Freccero M, Gandolfi R, Sarzi-Amadè M, Rastelli A (2000) Facial selectivity in epoxidation of 2-cyclohexen-1-ol with peroxy acids. A computational DFT study. J Org Chem 26:8948–8959

48. Mason JA, Veenstra M, Long JR (2014) Evaluating metal–organic frameworks for natural gas storage. Int J Chem Sci 1:32–51

49. Sheldon R, Van Doorn J (1973) Metal-catalyzed epoxidation of olefins with organic hydroperoxides: I. A comparison of various metal catalysts. J Catal 3:427–437

Publisher's Note Springer Nature remains neutral with regard to jurisdictional claims in published maps and institutional affiliations.